



## Research Paper

## Photothermal effects of gold nanoparticles induced by light emitting diodes

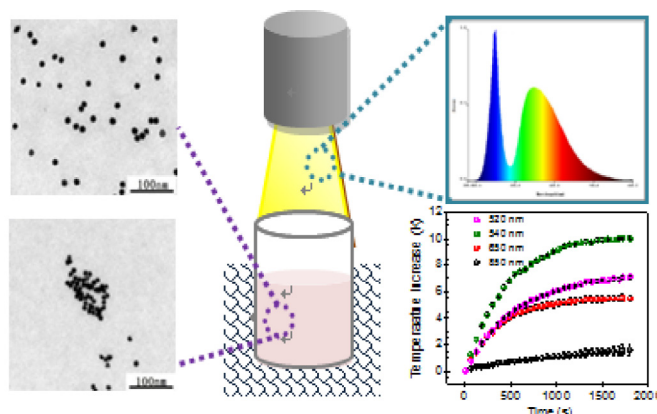
Kai Yue<sup>\*</sup>, Jingyang Nan, Xinru Zhang, Jue Tang, Xinxin Zhang

School of Mechanical Engineering, University of Science and Technology Beijing, Beijing 100083, China

## HIGHLIGHTS

- Feasibility of LED using for localized heating of treated biological media is proven.
- Possible mechanism for effect of key factors on temperature rise is deeply analyzed.
- AuNP aggregation is observed in biological media and causes decrease in temperature.
- Major determinant of LED photothermal effect for blood and tissue is determined.
- Smaller-size, higher concentration, and higher power density increase temperature.

## GRAPHICAL ABSTRACT



## ARTICLE INFO

## Article history:

Received 27 November 2015

Accepted 14 January 2016

Available online 6 February 2016

## Keywords:

Biological tissue

Gold nanoparticle (AuNP)

Light emitting diode (LED)

Photothermal effect

Temperature increase

## ABSTRACT

Gold nanoparticles (AuNPs) have a great potential for biomedical application due to the superior photothermal efficiency. The photothermal effects of AuNPs in different heated media under a polychromatic and three monochromatic light emitting diode (LED) illuminations were experimentally investigated to explore the possible use of LED for the thermotherapy treatment. The results show that the noticeable temperature increase of the heated media can be achieved by the injection of AuNPs induced by LED illumination. The selection of the LED wavelength depends not only on the absorption peak wavelengths of the AuNP with different sizes but also on the absorption coefficient of the heated media. Either a smaller AuNP size, higher AuNP concentration, or higher power density can lead to a higher temperature increase. The AuNP aggregation occurred in the heated egg white, agar solution, and blood leads to the lower temperature increase comparing with the heated water. Moreover, the LED light with a wavelength of 635 nm results in better heating for the heated blood and biological tissue in vitro comparing with other selected wavelengths due to the lower light absorption of the blood, deeper penetration in biological tissues, and the light absorption rate of AuNP to a certain degree.

© 2016 Elsevier Ltd. All rights reserved.

## 1. Introduction

The nanoparticle technology has become increasingly attractive for biomedical and biotechnological applications in recent years.

Gold nanoparticle (AuNP) has received lots of attention for various uses by taking advantage of the unique spectral and surface properties. It may turn out to be a key breakthrough in cancer hyperthermia treatment because it can efficiently converts the absorbed light to heat energy by surface plasma resonance for localized heating in target tumor tissue and can be easily bioconjugated with peptides, antibodies and small molecules [1,2]. During thermal therapy, the accurate control of temperature in the targeted tumor

<sup>\*</sup> Corresponding author. Tel.: +86 10 62332743; fax: +86 10 62332743.

E-mail address: [yuekai@ustb.edu.cn](mailto:yuekai@ustb.edu.cn) (K. Yue).

tissue is crucial for successful cancer treatment. Therefore, a deep understanding of the photothermal properties of AuNPs plays a significant role in both the fundamental research and the future biomedical application.

Up to now, there have been a lot of investigations on the photothermal properties of the AuNPs. Hainfeld et al., Visaria et al. and Huang et al. studied the feasibility of photo-thermal tumor therapy using AuNPs under laser light illumination [3–5]. Lin et al. observed a near-surface temperature increase of 10 °C under the laser illumination at 808 nm and 852 nm [6]. Roper et al., Cole et al., and Qin et al. conducted experiments to obtain the effects of laser power, the dimension and shape of AuNPs on the photothermal conversion efficiency [7–9]. Xie et al. investigated the effects of the amount of energy and pulse energy on the maximum temperature, rate of temperature increase, and localized heating [10]. An et al. and Ekaterina et al. studied the effects of the particle concentration, laser power, particle size and shape, and the initial temperature of particles on the temperature distribution and rate of temperature increase [11,12]. Govorov et al. demonstrated that the amount of generated heat and temperature increase depends on the number of nanoparticles in a complex [13]. Richardson et al. determined the efficiency of light-to-heat conversion and revealed main mechanism of thermal equilibration [14]. Henglein and Dan measured the relationship of the plasmon absorption band of AuNPs and the particle size [15].

Due to the excellent monochromaticity, high intensity, strong directivity, and good coherence of the laser light, most recent studies have been done using laser as the light source to excite the localized surface plasmon of the AuNPs. However, the collimation of fine laser beam often leads to a non-uniform heat distribution within an irregular treated tumor tissue. The high cost, complicated structure, difficult-to-maintain, and relatively short lifetime of the laser therapy devices suggest the possibility of finding other good light sources in this area. Comparing with the laser light, the light emitting diode (LED) has some special advantages, such as low energy consumption, longer lifetime, lower cost, safe to use, and being readily applicable. Moreover, the power conversion efficiency of LED can be higher than 90%. Thereby, the LED technology has been developed rapidly, which expedites the investigation on the potential application of LED as an alternative light source in biomedical research and clinical practice.

Whelan et al. successfully measured 50–86% cell kill in vitro using LED with a peak emission of 728 nm and 680 nm as a light source

in photodynamic therapy [16]. Schmidt et al. conducted a comparison of brain stem toxicity in canines and concluded that LEDs are a suitable light source for photodynamic therapy of brain tumors with photofrin [17]. If the LED could be used as a light source in practice, the multiple micro-scale LEDs may be placed in the subcutaneous tissue or located in the body cavities close to the treated tissue while the laser light is transmitted through an optical fiber in laser photothermal therapy. Daly et al. developed a novel LED array to treat large bulky tumors by encapsulating LEDs within biocompatible silicon for interstitial placement within the treatment tissue, and carried out preliminary non-clinical experiments in normal swine muscle and demonstrated a significant treatment zone [18].

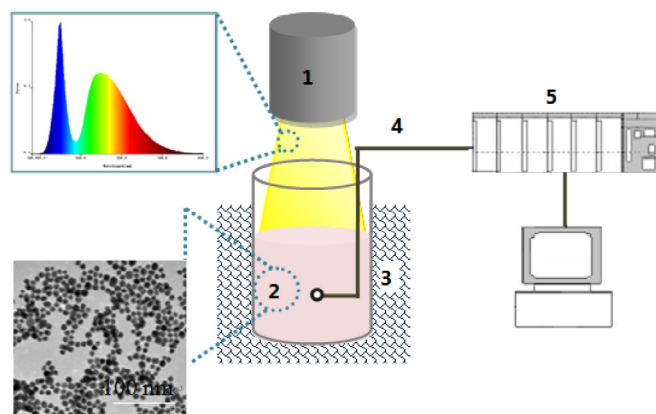
The aim of the present study is to explore the possibility of using LED as the light source for AuNPs-mediated thermal therapies in the future practical application. The experimental system was designed and established to measure the temperature increase of the heated media injected with the AuNP solution for determining the photothermal effect of the AuNPs in different media. Furthermore, the effects of the AuNP size and concentration, power density, and LED wavelength were analyzed.

## 2. Experimental measurement

### 2.1. Experimental system

Fig. 1 shows the schematic diagram of the experimental system used to quantify the LED induced photothermal effect of AuNPs in different heated media. There are five major components, including LED light source with different power densities and wavelengths, AuNP solution with different concentrations and particle sizes, thermal insulating materials, T-type thermocouples, and MX100 data collector.

In this experimental system, the AuNP solution was injected into the heated medium in a 25 mL beaker. The thermocouples were used to measure the temperature variation of the heated media under the LED illumination and the room temperature. The thermocouple was located 2 mm beneath the surface of the solution. The distance between the LED light and the test sample was 40 mm. The temperature signals were sampled every 500 ms by a MX100 data collector. In order to reduce the error, a reflecting shade surrounding the LED light source was employed to avoid the light leakage



1-LED light; 2-Heated media with AuNPs; 3-insulation; 4-Thermocouple; 5-MX100 Data Acquisition Unit and Computer.

Fig. 1. Schematic diagram of the experimental system.

**Table 1**  
Experimental factor and levels.

| Factor                   | Level 1              | Level 2              | Level 3              | Level 4 |
|--------------------------|----------------------|----------------------|----------------------|---------|
| Size (nm)                | 15                   | 25                   | 35                   |         |
| Heated media             | Agar                 | Egg white            | Blood                | Muscle  |
| NP concentration (mol/L) | $7.7 \times 10^{-4}$ | $3.4 \times 10^{-4}$ | $1.7 \times 10^{-4}$ |         |
| Light power (W)          | 3                    | 5                    | 7                    |         |
| Light wavelength (nm)    | 521                  | 635                  | 850                  | 420–540 |

and the insulating material was applied to make sure of an adiabatic environment. All experiments were conducted at the room temperature of 22–25 °C.

## 2.2. Preparation and characterization of the materials

The experimental factors and corresponding levels were selected in this study as shown in Table 1. The wavelength of the LED

light can significantly affect the temperature increase of the heated media. Considering the absorption peak of the AuNPs with different sizes, light intensities of the LED light, and the depths of light penetration in biological tissues, three monochromatic LED lights with the spectral bands around 521 nm, 635 nm and 850 nm and one polychromatic LED light with the wavelength in the range of around 420–540 nm were applied in this study [19]. We analyzed the emission spectra of these four LED light sources using an Ocean Optics reflectance spectrometer (USB4000), as shown in Fig. 2(a)–(d), respectively. When measuring the emission spectra, just a portion of the light beam was used to determine the spectral energy distribution of the LED light.

In order to accurately control the LED power in phototherapy, it is desired to investigate the relationship between the photothermal effect of AuNPs and the LED power density for the correct selection of LED light source in possible biomedical practice. In this experiment, three power densities, i.e., 9 mW/cm<sup>2</sup>, 15 mW/cm<sup>2</sup> and 21 mW/cm<sup>2</sup> were employed to investigate the effects of the LED

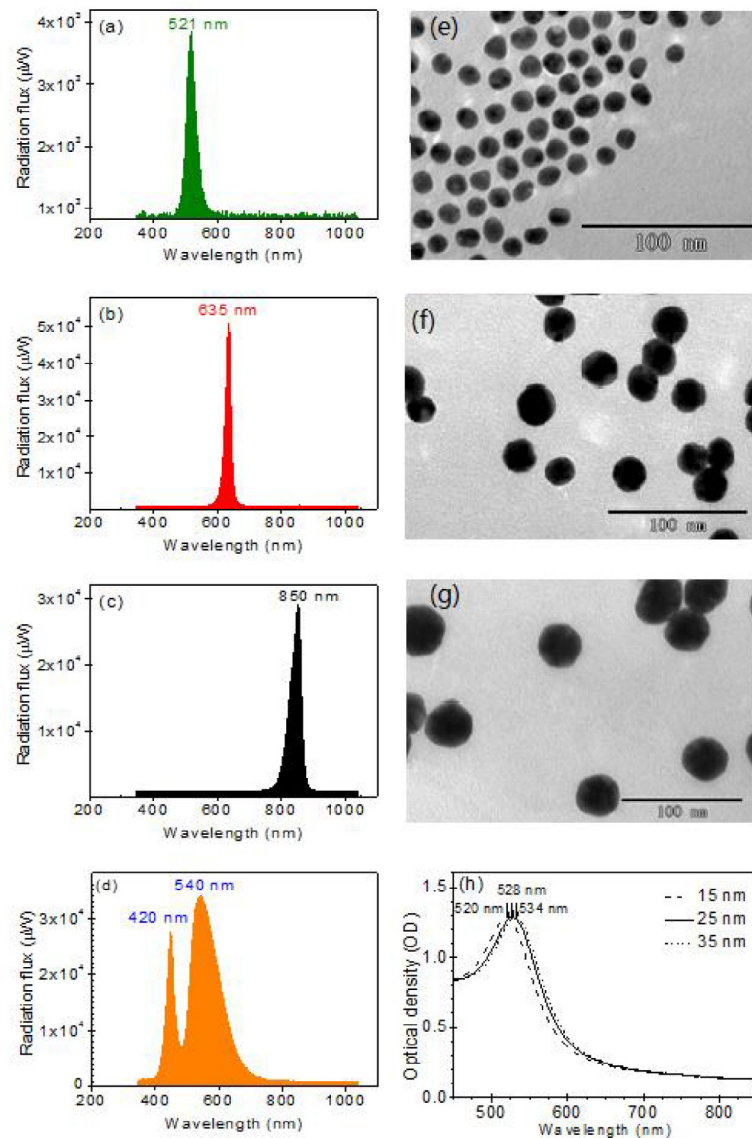


**Fig. 2.** Spectral characteristics of the LED light sources, (a) 521 nm; (b) 635 nm; (c) 850 nm; (d) polychromatic LED light; TEM images of AuNPs, (e) 15 nm; (f) 25 nm; (g) 35 nm; and (h) characteristic spectrum for the AuNPs of 15 nm, 25 nm, and 35 nm.

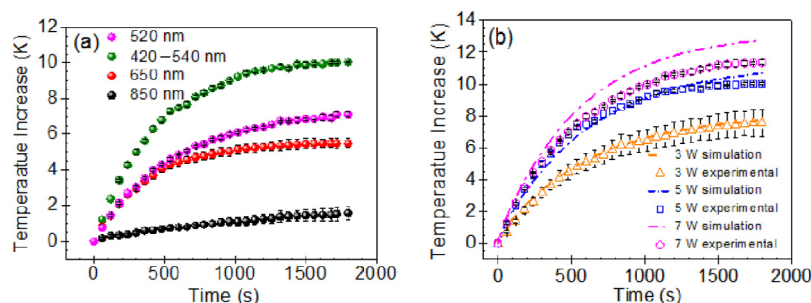


Fig. 3. Effects of the factors on the temperature increases of heated media, (a) LED wavelength; (b) output power.

power density on the temperature increase of the heated water solution according to the related literatures [6,7,14,20].

Some of the AuNP sizes used for photodynamic therapy in biomedical investigations normally range from 5 nm to 50 nm [20–23]. Three nanoparticle diameters (15 nm, 25 nm, and 35 nm) were selected to investigate the photothermal effect of AuNPs in this work. The 15 nm diameter spherical AuNPs were produced by the colloidal chemical synthetic procedures with the use of sodium citrate as a stabilizing agent, and the 25 nm and 35 nm spherical AuNPs were made by seed crystal growth method based on the 15 nm gold nanoparticle solution. The TEM images of 15 nm, 25 nm, and 35 nm AuNP measured by a JEM-1200EX are shown in Fig. 2(e)–(g), respectively, from which the good uniformity in nanoparticle size distribution can be observed. The AuNP volume concentration in the different solutions with different size AuNPs were equivalent. Moreover, three AuNP concentrations, i.e.,  $7.7 \times 10^{-4}$  mol/L,  $3.4 \times 10^{-4}$  mol/L,  $1.7 \times 10^{-4}$  mol/L, were used during the experiment by referring to the related literature [5]. The absorbance values of the 15 nm, 25 nm, and 35 nm AuNP solution at the concentration of  $7.7 \times 10^{-4}$  mol/L were measured using a BIOTEK microplate spectrophotometer, as shown in Fig. 2(h). It is indicated that the absorption peak values are 520 nm, 528 nm, and 534 nm for the 15 nm, 25 nm, and 35 nm AuNPs.

Moreover, to investigate the photothermal effects of AuNPs under LED illumination in various biological tissues for possible biomedical application, the experimental measurements of the temperature increases of the agar solution, egg white solution, goat blood, and pig skeletal muscle in vitro were carried out when the AuNPs were injected under the same experimental conditions. The agar solution with the agar concentration of 15% was produced by mixing the agar powder with deionized water and being heated to 120 °C with a pressure cooker. The goat blood anticoagulated with sodium citrate was employed as the heated blood in this experiment. At the beginning of the experiments, 1 mL of  $7.7 \times 10^{-4}$  mol/L AuNP solution was manually added into the 1 mL of 15% agar solution, or the 1 mL of egg white solution, or 1 mL of goat blood, or deionized water solution by a 2 mL standard syringe, respectively. For the pig skeletal muscle in vitro, we used a controlled micro-volume syringe pump to inject 1 mL of  $7.7 \times 10^{-4}$  mol/L AuNP solution into it.

### 2.3. Implementation of the experiment

During experiment, a T-type thermocouple was firstly fixed in a 15 mL beaker and the heated medium was put into the beaker. Then, 1 mL AuNP solution with a certain concentration was injected into the heated media and the MX100 data collector was turned on for monitoring the temperature variation of the heated medium. Approximately 1 hour was required to intensively mix the solution with the heated medium and to reach thermal equilibrium. The baseline data were acquired at this point in time for half

an hour. Afterward, the LED light was turned on to illuminate the medium injected with the AuNP solution, and turned off after 30 min LED illumination. Each case was repeated three times and the results were averaged. Before the experiments began, the T-type thermocouples used for the temperature measurement have been calibrated by a standard thermometer and the instrument error of the data collector is 0.05 °C.

For the convenience of analysis and explanation, the temperature increase  $\Delta T_1$  above the baseline temperature of the heated medium under the LED illumination was firstly recorded when there are no any AuNPs in the medium, and then the temperature increase  $\Delta T_2$  above the baseline temperature of the heated medium injected with the AuNP solution was measured under the LED illumination. In the subsequent discussion, we used the temperature difference  $\Delta T$  between the  $\Delta T_2$  and  $\Delta T_1$  to analyze the photothermal effect of the AuNPs on the heated media. Furthermore, the use of  $\Delta T = \Delta T_2 - \Delta T_1$  is helpful to eliminate some probable errors in the experimental measurement.

## 3. Results and discussion

### 3.1. Effects of the LED wavelength and power density

Fig. 3(a) shows the temperature increases of the water solution injected with the 15 nm AuNPs at  $7.7 \times 10^{-4}$  mol/L concentration and 15 mW/cm<sup>2</sup> power density when the wavelengths of the LED lights are around 521 nm, 635 nm, 850 nm, and 420–540 nm, respectively. It is found that after heating for 30 min, the temperature increase of the heated water solution at 635 nm is 5.5 °C, which is only a half of that at 420–540 nm, i.e., 10.05 °C, and is also smaller than the 7.1 °C increase in temperature at 521 nm. The temperature increase at 850 nm is even smaller, only 1.58 °C.

One reason for this phenomenon is that the AuNP has a lower rate of absorption for the LED light at 635 nm wavelength than that at the wavelengths of 420–540 nm and 521 nm, and has the lowest rate of absorption at 850 nm wavelength for the AuNPs with the diameters of 15 nm, 25 nm, and 35 nm, which can be concluded from the absorption spectra of the AuNPs at different wavelengths as shown in Fig. 2(h). As a result, the temperature increase of the heated water solution will decrease with the increase of the light wavelength within the range of around 420–850 nm. Another notable finding is that the temperature increase of the heated medium under the polychromatic LED light illumination within the wavelength range of 420–540 nm is significantly higher than that under the monochromatic LED light illumination at the wavelength of 521 nm due to the more light energy absorbed by AuNPs in the former case. That means that if there is similar absorption peak value, the polychromatic light would be the better choice compared with the monochromatic light for localized heating in biomedical application. It is also for this reason that some of the following experiments were carried out using the 420–540 nm LED light.



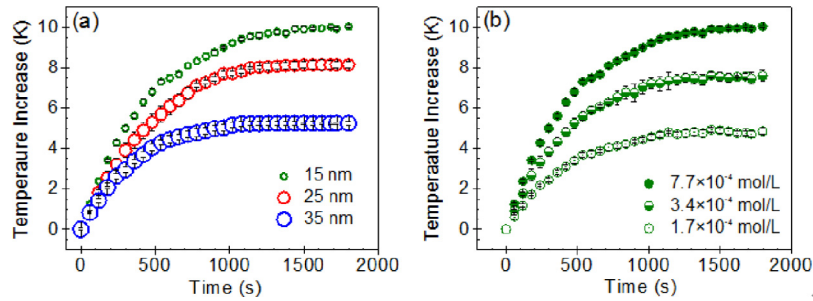


Fig. 4. Effects of the factors on the temperature increases of heated media, (a) nanoparticle size; (b) nanoparticle concentration.

When the AuNP concentration, AuNP size, and the LED wavelength were set to  $7.7 \times 10^{-4}$  mol/L, 15 nm, and 420–540 nm, respectively, the temperature increases of the heated water solution under LED illumination at different power densities are shown in Fig. 3(b). It is indicated that the temperature differences  $\Delta T = \Delta T_2 - \Delta T_1$  after heating for 30 min are 7.6 °C, 10.1 °C, and 11.4 °C at power densities of 9 mW/cm<sup>2</sup>, 15 mW/cm<sup>2</sup>, and 21 mW/cm<sup>2</sup>, respectively, and the temperature increase caused by the AuNPs at the power density of 21 mW/cm<sup>2</sup> remains the largest value at different time points. The major reason for this phenomenon may be explained by the heat generation produced by all AuNPs, which is referred to as specific absorption rate (SAR) and is expressed as [9]

$$\text{SAR} = N \cdot C_{\text{abs}} \cdot I_a = N \cdot Q_{\text{nano}} \quad (1)$$

where  $N$  represents the total number of the AuNPs,  $C_{\text{abs}}$  represents the absorption cross-section area of each AuNP, which is an effective area that absorbs the light energy impinging upon the AuNP,  $I_a$  represents the light power density, and  $Q_{\text{nano}}$  represents the amount of heat generated by each AuNP.

Thus, as can be seen from Eq. (1), because the light power density  $I_a$  increases with the increase of the LED power density, the heat energy produced by each AuNP will subsequently increase under the same experimental conditions. In such a way, a higher power density could lead to a higher temperature increase of the heated medium. Moreover, it is worthy of notice that comparing the temperature differences at 15 mW/cm<sup>2</sup> and 21 mW/cm<sup>2</sup> power densities with that at 9 mW/cm<sup>2</sup>, the increasing ratios of the temperature differences at 15 mW/cm<sup>2</sup> and 21 mW/cm<sup>2</sup> to that at 9 mW/cm<sup>2</sup> are 33% and 50%, respectively, while the increasing ratios of 15 mW/cm<sup>2</sup> and 21 mW/cm<sup>2</sup> to the 9 mW/cm<sup>2</sup> are 67% and 133%. Obviously, the increasing ratios of the temperature differences are smaller than that of the power density. Furthermore, the difference between the increasing ratio of the temperature difference and the increasing ratio of the power density at 15 mW/cm<sup>2</sup> is larger than that at 21 mW/cm<sup>2</sup>. This is most likely due to the fact that a higher LED power density leads to a higher temperature of the experimental system and a larger amount of heat will lose to the environment.

The corresponding numerical simulation was carried out using FLUENT software for obtaining the photothermal effect of the AuNPs in water solution to better understand how the LED power density affects the temperature increase of the heated medium. By calculating the absorbance of the 15 nm AuNP solution with a concentration of  $7.7 \times 10^{-4}$  mol/L according to the method listed in Ref. 14, it can be obtained that the AuNPs absorb around 22% of the LED light. In the simulation, the photothermal conversion efficiency by the AuNPs was assumed to be constant and the photoelectric conversion efficiency of the LED light was assumed to be 15% in consideration of a large heat loss. The comparison of the temperature increases between the calculated results and experimental data, as shown in Fig. 3(b), indicates that the calculated temperature differences  $\Delta T$  after heating for 30 min at the power densities of 9 mW/

cm<sup>2</sup>, 15 mW/cm<sup>2</sup>, and 21 mW/cm<sup>2</sup> are 7.7 °C, 10.7 °C, and 12.7 °C, respectively. As can be seen, there is a good agreement between the calculated results and experimental data at the power density of 9 mW/cm<sup>2</sup>, but the calculated results do not agree very well with the experimental data at the power densities of 15 mW/cm<sup>2</sup> and 21 mW/cm<sup>2</sup>. The difference between the calculated results and experimental data at 21 mW/cm<sup>2</sup> power density is larger than that at 15 mW/cm<sup>2</sup> power density. One reason for this phenomenon is that the heat loss from the LED with higher power density is more than that with lower power density under the same conditions in the practical experiments. In the simulation, the heat loss from the LED during the heating period was assumed to be a constant value in this study while in fact it changes with temperature of the LED system to a certain extent.

### 3.2. Effects of the nanoparticle size and nanoparticle concentration

When the AuNP concentration was set to  $7.7 \times 10^{-4}$  mol/L, the power density was 15 mW/cm<sup>2</sup>, and the wavelengths of the LED light was 420–540 nm, the temperature difference between the temperature increases of the heated water solution with injected AuNP solution and that without AuNPs under different NP size conditions was shown in Fig. 4(a).

It can be observed that the temperature increase  $\Delta T_2$  of the water solution injected with the AuNPs under LED illumination is higher than the temperature increase  $\Delta T_1$  of the water solution without AuNPs by 10.05 °C, 8.15 °C, and 5.25 °C when the nanoparticle size is 15 nm, 25 nm, and 35 nm, respectively. That means that an increase in the AuNP size leads to substantial decreases in the temperature difference  $\Delta T = \Delta T_2 - \Delta T_1$  and temperature increase  $\Delta T_2$  of the heated medium with injected AuNPs. Moreover, the temperature difference  $\Delta T$  and the temperature increases  $\Delta T_2$ ,  $\Delta T_1$  all exponentially increase with time, i.e., the growth rate of the temperature increases rapidly at the beginning of time period and then becomes smaller over time, and the temperature increase will reach a steady state faster for the larger nanoparticles, but stabilize at a lower temperature increase. It can be explained that when the gold content in the heated medium is the same in each experiment under the different AuNP size conditions, the total volume  $V$  of AuNPs remains constant. If the diameter of a larger AuNP with the constant volume  $V$  is  $R_1$ , and that of the  $N$  smaller AuNPs is  $R_2$ , then we get the equation  $V = 4/3\pi R_1^3 = N \cdot 4/3\pi R_2^3$  and  $R_1/R_2 = N^{1/3}$ . So the absorption cross-section area that absorbs the light energy for the larger AuNP could be  $S_1 = \pi R_1^2 = \pi R_2^2 \cdot N^{2/3}$ , and that for the smaller AuNPs is  $S_2 = \pi R_2^2 \cdot N$ . Comparatively, the smaller AuNP size will result in a larger total absorption cross-section area because of  $N > N^{2/3}$ . If  $I_a$  remains the same for each experimental measurement, the total amount of light energy absorbed by all smaller AuNPs should be larger than that absorbed by all larger AuNPs according to eq. (1). Therefore, the temperature increase of the heated medium with smaller AuNPs is higher than that caused by larger AuNPs.

Another reason is that different AuNP sizes can lead to obvious change to the photothermal conversion efficiency of the AuNPs and an increase in AuNP size will result in a decrease in the efficiency [24]. The photothermal conversion efficiencies of the AuNPs with the diameters of 15 nm, 25 nm, and 35 nm are 0.9, 0.86, and 0.73, respectively, according to the experimental results from Ref. [25]. This is because that the AuNPs can both absorb and scatter light and the photothermal conversion efficiency of AuNPs is determined by the fraction of the absorption in the extinction, which is the sum of the absorption and scattering. Studies show that the increase in the particle size causes in an increase in the extinction cross section as well as the relative contribution of scattering [26]. Subsequently, the lower photothermal conversion efficiency of the AuNPs with larger diameter due to the greater scattering effect also results in the lower temperature increase of the heated media.

Fig. 4(b) shows the temperature increases of the water solution injected with AuNPs at different AuNP concentrations when the AuNP size, the LED power density, and LED wavelength were set to 15 nm, 15 mW/cm<sup>2</sup>, and 420–540 nm, respectively. It is found that higher AuNP concentration results in the larger temperature increase. The final temperature increases at the AuNP concentration of  $7.7 \times 10^{-4}$  mol/L,  $3.4 \times 10^{-4}$  mol/L,  $1.7 \times 10^{-4}$  mol/L are 10.05 °C, 7.63 °C, and 4.93 °C, respectively. The rate of change in temperature increase of the heated medium is smaller during the initial period of heating at the lower AuNP concentration. Moreover, the temperature increase at the lower AuNP concentration reaches equilibrium more quickly. This can be explained by eq. (1) that the heat generation produced by all AuNPs at higher AuNP concentration is larger because the number of the AuNPs per unit volume increases.

### 3.3. The photothermal effects of AuNPs in different media

The temperature differences  $\Delta T = \Delta T_2 - \Delta T_1$  of the different heated media injected with 15 nm AuNPs under 15 mW/cm<sup>2</sup> LED light illumination at 420–540 nm and 635 nm wavelength are shown in Fig. 5(a) and 5(b), respectively, while the AuNP concentration was set to  $3.4 \times 10^{-4}$  mol/L. Firstly, it can be seen that the temperature difference of the water solution caused by the injected AuNPs is the highest among those of all other tested media at the wavelengths of both 420–540 nm and 635 nm. This is mostly because the existence of the various ions in the agar solution, egg white, and goat blood may promote the aggregation of the AuNPs. Moreover, the interaction of the AuNPs with various proteins in the agar solution, egg white, and goat blood can change the characteristics of the surface plasmon resonance of AuNPs and promotes the AuNP aggregation [27,28]. In order to confirm the occurrence of the AuNP aggregation in the different heated media employed in this study, the TEM images were recorded with a JEM-1200EX. Fig. 5(d)–(g) shows the TEM images of the AuNP distribution in the water, agar, white egg, and blood solutions after mixing 1 mL AuNP solution with 1 mL heated medium at the room temperature for 1 hour, respectively. It can be clearly seen that the AuNPs are uniformly distributed in the water solution, as shown in Fig. 5(d), but the obvious AuNP aggregates have formed in the agar, white egg, and blood solutions, as shown in Fig. 5(e)–(g), respectively.

The heat generation of the AuNPs would subsequently be affected and the temperature increase of the heated organic media changes due to the occurrence of the AuNP aggregation. The temperature increase would decrease and drops more sharply if the number of the aggregating AuNPs increases according to the following Eq. (2) [9].

$$\Delta T_{red} = \Delta T / N_{NP}^{2/3} R_{eff}^2 \sim N_{NP}^{2/3} \quad (2)$$

where  $\Delta T$  and  $\Delta T_{red}$  represent the temperature increase occurred before and after the AuNP aggregation, respectively;  $N_{NP}$  repre-

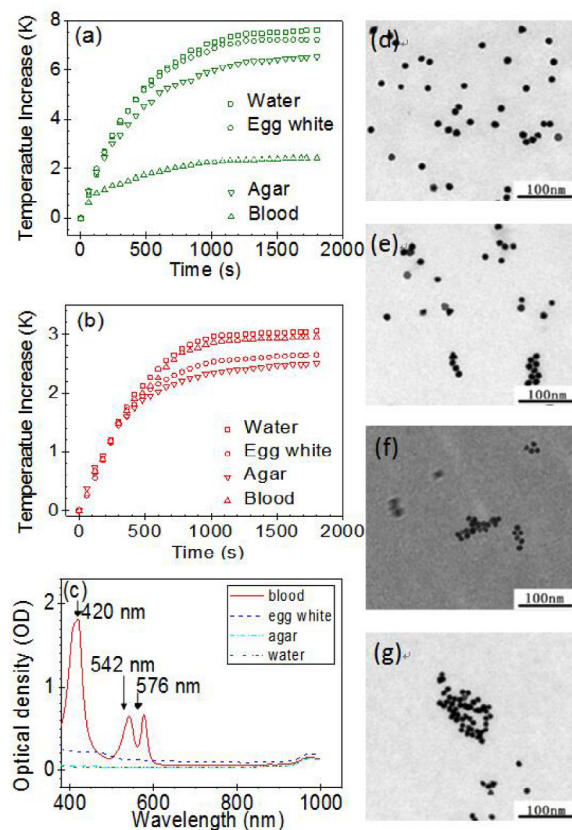


Fig. 5. Temperature increases as a function of time for the four heated media, (a) 420–540 nm polychromatic LED light; (b) 635 nm monochromatic LED light; (c) characteristic spectrum for the heated media; TEM images for the nanoparticles in the four heat media: (d) water; (e) egg white; (f) agar; (g) blood.

sents the number of the aggregated AuNPs; and  $R_{eff}$  represents the radius of the AuNP aggregate.

Secondly, it is found from Fig. 5(a) and 5(b) that the temperature increase of the egg white solution is higher than that of the agar solution at the wavelengths of both 420–540 nm and 635 nm, and the difference of the temperature increases between the water solution and goat blood changes a lot at different wavelengths, which is 5.22 °C at 420–540 nm while 0.1 °C at 635 nm. One possible explanation for this occurrence is that the heat capacity of the 0.15% agar solution (4.177 kJ/(kg·K) [29]) is larger than that of the egg white (3.7 kJ/(kg·K) [30]) while the thermal conductivities of the agar solution and egg white are similar. The blood has different absorptions at different wavelengths. The absorption spectra of the water, egg white, agar solution, and goat blood were measured with a BIOTEK microplate spectrophotometer (EPOCH), as shown in Fig. 5(c). It is clear that there is no high absorption peak for the water, egg white, and agar solutions in the wavelength range of 400–900 nm concerned in this study. But the blood absorbs around 24% of the light at 540 nm wavelength while nearly 0 at 635 nm wavelength if converting to the rate of absorption. Thus, less light energy could be absorbed by the AuNPs due to more light energy absorbed by the blood at the wavelengths of 420–540 nm comparing with 635 nm, and subsequently the temperature increase of the blood injected with AuNPs at 635 nm is higher than that at 420–540 nm.

Moreover, the temperature increases of the heated media at the wavelengths of 420–540 nm are mostly higher than that at 635 nm due to the higher rate of absorption of the AuNPs for the LED light at the wavelengths of 420–540 nm. The light absorbed by the water

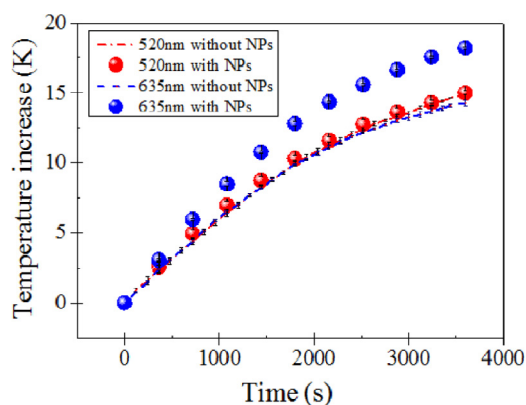


Fig. 6. The temperature increases of the heated pig skeletal muscle in vitro.

solution is only 0.012% and 0.074% at the wavelength of 540 nm and 635 nm [31], which is so small that can be neglected and has a little effect on the temperature increase. Similarly, the light absorbed by the blood at 635 nm can be negligible. That is why the difference of the temperature increases between the water solution and the blood is just 0.1 °C at 635 nm.

As mentioned above, the temperature increase caused by the injected AuNPs depends not only on the absorption band of AuNPs but also on the absorption spectrum of the heated media. It was found that the amount of the light that penetrates the sample is larger and the reaching distance of the light is deeper at the wavelength of 635 nm comparing with 520 nm [32]. In this study, the temperature measurements were carried out for the pig skeletal muscle tissues injected with 15 nm AuNPs and without AuNPs, respectively, at  $7.7 \times 10^{-4}$  mol/L concentration. The thermocouple was located approximately 5 mm beneath the surface of the pig skeletal muscle tissue. Fig. 6 shows the temperature increases of the heated pig skeletal muscle tissues under 15 mW/cm<sup>2</sup>, 520 nm and 635 nm LED light illumination. The results of the temperature measurement of the pig skeletal muscle tissues under 15 mW/cm<sup>2</sup>, 520 nm LED light illumination indicate that there is almost no difference in the temperature increase between the pig skeletal muscle tissue injected with AuNPs and without AuNPs. After illuminating by the 635 nm LED light for 1 hour, the temperature increase is 14.3 °C for the pig skeletal muscle tissue without AuNPs, but is 18.2 °C (27% increase) for the pig skeletal muscle tissue injected with AuNPs. This suggests that a marked increase in the temperature of the heated biological tissue can be achieved by injecting AuNPs under the same light intensity condition, and correspondingly prove the possibility and effectiveness of the use of LED as a light source for potential biomedical application.

#### 4. Conclusion

The experimental measurements have been conducted in this study to evaluate the photothermal effect of the AuNPs under LED light illumination and to explore the possibility of using LED as the light source for hyperthermia treatment in the potential biomedical application. The temperature increases of the heated water, agar solution, egg white, blood, and pig skeletal muscle tissue and the possible mechanism for effect of key factors were deeply investigated under the different AuNP and LED conditions.

The results of this study conclude that it would be better to select the smaller particle size and higher AuNP concentration as much as possible within the selectable range in the practical biomedical application. For the wavelength selection of LED light source, the depth of light penetration in biological tissues and the absorption peak of the AuNPs should be taken into account at the same time.

The wavelength of around 635 nm would be a good option for increasing the temperature of the treated media due to the lowest absorption coefficient in the NIR window (600–900 nm) in vivo. However, the optimized LED wavelength should be reselected because the absorption peak wavelength of the AuNPs would have a right-shift with the increase of the AuNP size. The occurrence of AuNP aggregation due to the interaction of AuNPs with ions and proteins and its effect on the temperature increase of the heated media will be quantitatively investigated in future work. Although the measurement error existed in this experimental system cannot be neglected, the noticeable temperature increase caused by injection of AuNPs induced by LED illumination demonstrates the promising potential of LED for application in photothermal treatment.

#### Acknowledgements

This work was funded by the National Natural Science Foundation of China (Grant No. 51276013). The kind assistance and guidance from Dr. Hongliang Yan and Dr. Lingyun Zhao is also gratefully acknowledged.

#### References

- [1] I.H. El-sayed, X.H. Huang, M.A. El-sayed, Selective laser photo-thermal therapy of epithelial carcinoma using anti-EGFR antibody conjugated gold nanoparticles, *Cancer Lett.* 239 (2006) 120–135.
- [2] D.P. O'Neala, L.R. Hirsch, N.J. Halasc, Photo-thermal tumor ablation in mice using near infrared-absorbing nanoparticles, *Cancer Lett.* 209 (2004) 171–176.
- [3] J.F. Hainfeld, D.N. Slatkin, T.M. Focella, Gold nanoparticles: a new X-ray contrast agent, *Br. J. Radiol.* 79 (2006) 248–253.
- [4] R.K. Visaria, R.J. Griffin, B.W. Williams, Enhancement of tumor thermal therapy using gold nanoparticle-assisted tumor necrosis factor- $\alpha$  delivery, *Mol. Cancer Ther.* 5 (2006) 1014–1020.
- [5] P.K. Jain, X.H. Huang, I.H. El-Sayed, Noble metals on the nanoscale: optical and photothermal properties and some applications in imaging, sensing, biology, and medicine, *Acc. Chem. Res.* 41 (2008) 1578–1586.
- [6] J.T. Lin, Selective cancer therapy using IR-laser-excited gold nanorods, *SPIE, Newsroom*, 10.1117/2.1201006.002507, 1–3.
- [7] D.K. Roper, W. Ahn, M. Hoepfner, Microscale heat transfer transduced by surface plasmon resonant gold nanoparticles, *J. Phys. Chem. C Nanomater. Interfaces* 111 (2007) 3636–3641.
- [8] J.R. Cole, N.A. Mirin, M.W. Knight, Photothermal efficiencies of nanoshells and nanorods for clinical therapeutic applications, *J. Phys. Chem. C Nanomater. Interfaces* 113 (2009) 12090–12094.
- [9] Z.P. Qin, J.C. Bischof, Thermophysical and biological responses of gold nanoparticle laser heating, *Chem. Soc. Rev.* 41 (2012) 1191–1217.
- [10] B. Xie, R. Singh, F.M. Torti, Heat localization for targeted tumor treatment with nanoscale near-infrared absorbers, *Phys. Med. Biol.* 57 (2012) 5756–5775.
- [11] W. An, Q.Z. Zhu, T. Zhu, Radiative properties of gold nanorod solutions and its temperature distribution under laser irradiation: experimental investigation, *Exp. Therm. Fluid Sci.* 44 (2013) 409–418.
- [12] E.Y. Lukianova-Hleb, L.J.E. Anderson, L. Seunghyun, Hot plasmonic interactions: a new look at the photothermal efficacy of gold nanoparticles, *Phys. Chem. Chem. Phys.* 12 (2010) 12237–12244.
- [13] A.O. Govorov, H.H. Richardson, Generating heat with metal nanoparticles, *Nano Today* 2 (2007) 30–38.
- [14] H.H. Richardson, M.T. Carlson, P.J. Tandler, Experimental and theoretical studies of light-to-heat conversion and collective heating effects in metal nanoparticle solutions, *Nano Lett.* 9 (2009) 1139–1146.
- [15] A. Henglein, M. Dan, Control of the size of colloidal gold nanoparticles, *Langmuir* 14 (1998) 7392–7396.
- [16] H.T. Whelan, E.V. Buchmann, N.T. Whelan, NASA light emitting diode medical applications from deep space to deep sea, *AIP Conf. Proc.* 552 (2001) 35–45.
- [17] M.H. Schmidt, D.M. Bajic, K.W. Reichert, Light-emitting diodes as a light source for in traoperative photodynamic therapy, *Neurosurgery* 38 (1996) 552–557.
- [18] S.R. Daly, F. Zheng, M. Krouse, A novel LED array used for photodynamic therapy (PDT), *Proc. SPIE Int. Soc. Opt. Eng.* 4996 (2003) 229–234.
- [19] S. Jain, D.G. Hirst, J.M. O'Sullivan, Gold nanoparticles as novel agents for cancer therapy, *Br. J. Radiol.* 85 (2012) 101–113.
- [20] Y. Cheng, A.C. Samia, J.D. Meyers, Highly efficient drug delivery with gold nanoparticle vectors for in vivo photodynamic therapy of cancer, *J. Am. Chem. Soc.* 130 (2008) 10643–10647.
- [21] N. Juteau, W. Nayoun, J. Ho, pH-induced aggregation of gold nanoparticles for photothermal cancer therapy, *J. Am. Chem. Soc.* 131 (2009) 13639–13645.
- [22] X.H. Huang, I.H. El-Sayed, Q. Wei, Cancer Cell imaging and photothermal therapy in the near-infrared region by using gold nanorods, *J. Am. Chem. Soc.* 128 (2006) 2115–2120.

- [23] X.H. Huang, P.K. Jain, I.H. El-Sayed, Plasmonic photo thermal therapy (PPTT) using gold nanoparticles, *Lasers Med. Sci.* 23 (2008) 217–228.
- [24] K. Jiang, D.A. Smith, A. Pinchuk, Size-dependent photothermal conversion efficiencies of plasmonically heated gold nanoparticles, *J. Phys. Chem. C* 117 (2003) (2013) 27073–27080.
- [25] H. Chen, E. Al, Understanding the photothermal conversion efficiency of gold nanocrystals, *Small* 6 (2010) 2272–2280.
- [26] P.K. Jain, L.K. Seok, I.H. El-Sayed, Calculated absorption and scattering properties of gold nanoparticles of different size, shape, and composition: applications in biological imaging and biomedicine, *J. Phys. Chem. B* 110 (2006) 7238–7248.
- [27] S. Lazzari, D. Moscatelli, F. Codari, Colloidal stability of polymeric nanoparticles in biological fluids, *J. Nanopart. Res.* 14 (2012) 920–930.
- [28] S.H. Lacerda, J.J. Park, C. Meuse, Interaction of gold nanoparticles with common human blood proteins, *ACS Nano* 4 (2010) 365–379.
- [29] J.S.R. Coimbra, A.L. Gabas, L.A. Minim, Heat capacity and thermal conductivity of liquid egg products, *J. Food Eng.* 74 (2006) 186–190.
- [30] J. Fujino, T. Honda, Measurement of specific heat capacity of gelatin for human phantom using differential scanning calorimetry, in: *The 10th Asian Thermophysical Properties Conference*, 2013.
- [31] R. Deng, H.E. Yingqing, Y. Qin, Pure water absorption coefficient measurement after eliminating the impact of suspended substance in spectrum from 400 nm to 900 nm, *J. Remote Sens.* 16 (2012) 176–184.
- [32] R. Weissleder, A clearer vision for in vivo imaging, *Nat. Biotechnol.* 19 (2001) 327–331.